A Numerical Sensitivity Study of the Influence of Siberian Snow on the Northern Annular Mode

Y. PEINGS, D. SAINT-MARTIN, AND H. DOUVILLE

CNRM-GAME, Météo-France, and CNRS, Toulouse, France

(Manuscript received 14 January 2011, in final form 16 May 2011)

ABSTRACT

The climate version of the general circulation model Action de Recherche Petite Echelle Grande Echelle (ARPEGE-Climat) is used to explore the relationship between the autumn Siberian snow and the subsequent winter northern annular mode by imposing snow anomalies over Siberia. As the model presents some biases in the representation of the polar vortex, a nudging methodology is used to obtain a more realistic but still interactive extratropical stratosphere in the model. Free and nudged sensitivity experiments are compared to discuss the dependence of the results on the northern stratosphere climatology. For each experiment, a positive snow mass anomaly imposed from October to March over Siberia leads to significant impacts on the winter atmospheric circulation in the extratropics. In line with previous studies, the model response resembles the negative phase of the Arctic Oscillation. The well-documented stratospheric pathway between snow and the Arctic Oscillation operates in the nudged experiment, while a more zonal propagation of the signal is found in the free experiment. Thus, the study provides two main findings: it supports the influence of Siberian snow on the winter extratropical circulation and highlights the importance of the northern stratosphere representation in the models to capture this teleconnection. These findings could have important implications for seasonal forecasting, as most of the operational models present biases similar to those of the ARPEGE-Climat model.

1. Introduction

Snow cover is a key component of the climate system and has a strong influence on the energy and water budgets at the land surface. In consequence, snow anomalies represent a significant source of predictability for surface climate, particularly in spring, when the high snow albedo has the strongest impact on net surface radiation (Schlosser and Mocko 2003; Peings et al. 2011). Snow anomalies are also likely to trigger remote climate responses through atmospheric teleconnections. In particular, the influence of the Eurasian snow cover on the Asian monsoon has been extensively studied and is still a matter of debate (Hahn and Shukla 1976; Barnett et al. 1989; Peings and Douville 2010).

More recently, another important teleconnection has been highlighted between the autumn snow cover over Siberia and the subsequent wintertime extratropical atmospheric circulation in the Northern Hemisphere (Cohen and Entekhabi 1999; Cohen et al. 2001). There is observational evidence that the Siberian snow cover, particularly in October, is a good precursor of the Arctic Oscillation (AO; Thompson and Wallace 1998), which is also described as the northern annular mode (NAM). The snow cover extent also correlates well with the North Atlantic Oscillation (NAO), which is sometimes considered as a regional signature of the annular mode (Bojariu and Gimeno 2003). This lagged correlation has important implications for seasonal forecasting, as it could lead to improved forecasts of the AO–NAO and related phenomena. For example, Cohen and Fletcher (2007) used a simple statistical model to show the benefits of taking the Siberian snow cover into account to accurately predict the Northern Hemisphere surface temperature anomalies in winter. The physical explanation of this statistical relationship involves a relatively complex mechanism, first identified by Saito et al. (2001) in reanalyses and more precisely described by Cohen et al. (2007, hereafter C07). The six steps of this mechanism are as follows: 1) abnormally extensive snow is present over Siberia in early autumn; 2) the snow

Corresponding author address: Yannick Peings, CNRM/GMGEC/VDR, 42 avenue Gaspard Coriolis, 31057 Toulouse CEDEX 01, France.
E-mail: yannick.peings@cnrm.meteo.fr

DOI: 10.1175/JCLI-D-11-00038.1

anomaly creates a strong thermal forcing at the surface, reinforcing the climatological Siberian high that develops during this season; 3) in line with the planetary waves theory, the baroclinic response to snow increases the upward propagation of stationary waves from the troposphere over this region, which is characterized by a strong stationary wave activity (Plumb 1985); 4) at the end of autumn and/or in early winter, the polar night jet is weakened by the absorption of waves that propagate into the stratosphere, leading to a polar warming favored by the intrusion of midlatitude air masses in the vortex ; 5) in line with Baldwin and Dunkerton's (2001) findings, the annular zonal wind anomaly propagates downward; 6) several weeks later, the hemispheric signal reaches the surface and projects onto the negative AO pattern, with a positive anomaly centered over the polar cap region surrounded by negative anomalies over the North Atlantic and North Pacific regions. Conversely, a lack of snow over Siberia in autumn favors the positive phase of the AO. This teleconnection involving a stratospheric pathway could be implicated in the extreme cold events of winter 2009/10 (Cohen et al. 2010).

A few numerical experiments have successfully simulated this teleconnection with general circulation models (GCMs), thereby confirming the proposed stratospheric pathway between the Siberian snow and the northern winter atmospheric circulation. Gong et al. (2003a, hereafter G03) used the ECHAM3 model and prescribed contrasted snow anomalies over Siberia based on extreme values of observed snow extent in the autumn 1976 and 1988. In subsequent studies, the same authors pointed out that the regional features of Siberia, such as orography, the strong climatological stationary wave activity, and the thermally insulating effect of snow, were crucial in obtaining a significant response to the prescribed snow anomalies (Gong et al. 2003b, 2004b,a). Fletcher et al. (2009, hereafter F09) used the Geophysical Fluid Dynamics Laboratory atmosphere model version 2 and land model version 2 (GFDL AM2–LM2) to run two ensembles of seasonal simulations with low and high snow over Siberia. In particular, they emphasized the importance of the initial stratospheric conditions for the polar vortex response. Orsolini and Kvamstø (2009) used satellite-derived snow cover areas, available since the end of 1966, to prescribe realistic snow boundary conditions in the climate version of the Action de Recherche Petite Echelle Grande Echelle (ARPEGE-Climat) GCM. They found a link between snow and the Aleutian Icelandic low seesaw index (AIS; Honda et al. 2001) variability in late winter. More recently, Allen and Zender (2010) prescribed anomalous snow albedo over Eurasia in the National Center for Atmospheric Research Community Atmosphere Model, version 3 (NCAR CAM3) GCM. In response to this radiative forcing, a wave activity pulse propagated into the stratosphere, culminating in a negative phase of the Arctic Oscillation.

Hardiman et al. (2008) explored whether the current-generation coupled ocean–atmosphere GCMs were able to capture the snow–AO teleconnection. They found that all models used within the Coupled Model Intercomparison Project phase 3 (CMIP3) failed to represent such a relationship. They invoked two main reasons for this: 1) the snow forcing was insufficient, as the interannual snow variability simulated over Siberia was too weak; and/or 2) the snow-driven local atmospheric anomaly was too confined longitudinally, preventing sufficient wave activity in the stratosphere to weaken the polar vortex. Hardiman et al. (2008), as well as F09, also analyzed the sensitivity of the response to the vertical discretization in the stratosphere ("low top" and "high top" versions of AM2–LM2) and found no systematic improvement but significant differences, suggesting the importance of the model mean state to simulate the snow–AO relationship.

Consequently, up to now, some GCMs have shown an ability to simulate a realistic NAM response to Siberian snow anomalies; however, the majority of them do not reproduce it. The aim of the present study is to explore this question with the ARPEGE-Climat model to confirm the snow–AO relationship and to better understand why it is such a challenge for the current GCMs to capture this teleconnection. The focus is indeed on the strong dependence of the model response on the stratospheric climatology. For this purpose two pairs of simulations are compared: one with strong but common biases in the northern extratropical stratosphere, the other with a more realistic mean state obtained through a relaxation (or nudging) methodology.

The following section describes the ARPEGE-Climat atmospheric GCM, the nudging methodology, the sensitivity experiments to Siberian snow anomalies, and some diagnostic and statistical tools. Section 3 describes the results by distinguishing between the two sets (without and with nudging) of experiments, and the seasonal and monthly time scales. Finally, section 4 draws the main conclusions and discusses some prospects for future studies.

2. Methods

a. Model description

All simulations are performed with version 4 of the ARPEGE-Climat atmospheric GCM (Déqué et al. 1994) at a T63 truncation. Here we use a low-top configuration of the model with only 31 vertical levels and a lid at 10 hPa, since an increased vertical resolution in the stratosphere

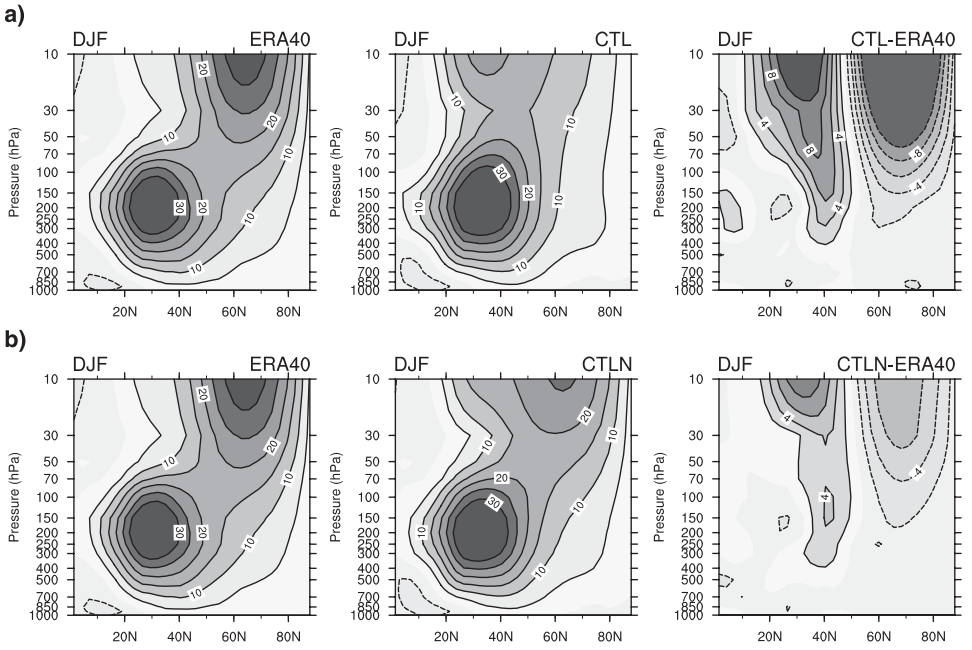

FIG. 1. (a) Zonal-mean zonal wind (m s^{-1}) for (left to right) ERA-40, the CTL experiment, and the difference CTL − ERA-40. (b) As in (a), but for the CTLN experiment. Period: 1971–2000.

does not improve the model climatology. The land surface component is the Interactions between Soil, Biosphere, and Atmosphere (ISBA) model with a single-layer snow model (Douville et al. 1995) and a simple force–restore scheme with improved subgrid hydrology (Decharme and Douville 2007). Unlike the original ISBA formulation, the bare ground snow cover fraction is diagnosed from snow water equivalent using the empirical relationship of Niu and Yang (2007) to improve both the climatology and the interannual variability of the Northern Hemisphere snow cover. The masking effect of the vegetation is still parameterized following Douville et al.'s (1995) formulation and ensured a reasonable surface albedo over forested areas. Finally, ISBA offers the possibility of exerting strong control on the land surface variables (here the simulated snow mass) through a simple nudging (i.e., relaxation) technique applied at each time step. This methodology is employed to prescribe a constant snow mass anomaly over Siberia (see section 2d).

b. Diagnostic and statistical tools

To diagnose the planetary wave activity induced by the prescribed snow anomalies, we use the 3D wave activity flux (WAF) of Plumb (1985), which is a generalization of the Eliassen–Palm (EP) flux (Andrews et al. 1987). It is computed using temperature, geopotential, and wind fields after removing their zonal mean.

To determine the significance of the differences between the perturbed experiments and their respective control simulations, we use a Student's *t* test computed from the 50-member ensemble available for each experiment.

c. Correction of the northern stratosphere mean state

1) MODEL BIASES (CTL EXPERIMENT)

Although ARPEGE-Climat is able to accurately reproduce some features of the extratropical atmospheric circulation, it shares a common bias with many other GCMs (Maycock et al. 2011) concerning the position and strength of the stratospheric polar night jet. This problem is illustrated in Fig. 1a, which shows the winter climatological zonal-mean zonal wind in the Northern Hemisphere for both the ARPEGE-Climat model and the 40-yr European Centre for Medium-Range Weather Forecasts Re-Analysis (ERA-40) (Uppala et al. 2005). This climatology comes from the control experiment with prescribed climatological SST [control (CTL)]. The polar night jet reaches its maximum intensity and variability in this season, when the vortex induced by low temperatures in the polar stratosphere is strongest. While the polar night jet is located between 60° and 80°N in ERA-40, it is too weak and displaced southward to around 40°N in the model.

2) NUDGING METHODOLOGY

This bias represents a serious limitation for our study, as the atmospheric response to the Siberian snow forcing is assumed to involve a stratospheric pathway and a

modulation of the polar vortex through wave–mean flow interactions. Thus, a good representation of the polar vortex mean state is crucial if such a teleconnection is to be analyzed. A recent study with ARPEGE-Climat (Saint-Martin et al. 2011, manuscript submitted to *Climate Dyn.*) shows that relaxing the equatorial stratosphere toward the ERA-40 leads to an improvement of the polar vortex climatology, with a more northward position and a greater intensity of the polar night jet. In line with these results, we chose to use the same nudging methodology here to assess whether a better simulation of the extratropical stratospheric mean state could alter the model response to the Siberian snow perturbation.

The nudging of the equatorial stratosphere is applied to horizontal wind components (u and v) and to temperature (T) at each time step. It is implemented by adding an extra term in the model prognostic equations as follows:

$$\frac{\partial X}{\partial t} = F(X) - \lambda(X - X_{\text{ref}}),$$

where X is the state of the model, X_{ref} is the reference field toward which the model is relaxed, and λ is the relaxation rate. The nudging intensity is maximum for the four highest levels ($\lambda = 1$ at 20, 40, 60, and 80 hPa) and gradually decreases for the three following levels (between 80 and 130 hPa) to ensure a smooth transition between the nudged and free layers of the atmosphere. The domain where the nudging is applied concerns only the stratospheric equatorial region between 15°S and 15°N, with a decreasing nudging strength across the boundaries of the domain.

As we perform sensitivity experiments, our aim is not to improve the interannual variability of the polar vortex but rather its mean state. Therefore, the equatorial stratosphere is nudged toward the ERA-40 *climatology* so that no interannual signal is introduced in the model. The 6-hourly climatological ERA-40 fields are interpolated linearly at the model time step (30 min) so that the nudging is as smooth as possible.

3) NEW CONTROL EXPERIMENT WITH NUDGING (CTLN)

The response of the extratropical atmospheric circulation is shown in Fig. 1b. In comparison with the free control run (CTL), the stratospheric polar night jet is shifted northward; the zonal wind maximum being located around 60°N. Although a part of the bias persists, the extratropical stratosphere climatology is now closer to ERA-40. Some complementary analyses suggest that most of the improvement is due to the temperature nudging rather than zonal and meridional wind nudging (not shown). The better temperature gradient in the equatorial stratosphere leads to a more realistic zonal wind structure in the extratropics, according to the thermal wind rule. Note that as the nudging is limited to the equatorial region, the extratropical atmosphere remains totally interactive and is only indirectly influenced by the model relaxation. Consequently, this nudging methodology is an efficient way to obtain a more realistic but still interactive extratropical stratosphere in our model.

4) IMPACT ON PLANETARY WAVE PROPAGATION

The evolution of the winter stratospheric polar vortex results from a complex interplay between radiative and planetary wave forcing [see Haynes (2005) for a review on stratospheric dynamics]. Vertically propagating waves originating from the troposphere interact with the stratospheric mean circulation and can initiate the phenomenon known as a sudden stratospheric warming (Matsuno 1971; Baldwin and Dunkerton 1989; Kodera and Chiba 1995; Polvani and Waugh 2004). Through simplified modeling and observations, it has been found that these vertically propagating waves occur only under certain atmospheric conditions. They are most prominent in the Northern Hemisphere winter under weak westerly wind conditions (Charney and Drazin 1961; waves propagate if $0 < U < U_c$, with U_c a critical value, depending on the wavenumber). Only the longest waves—that is, wavenumbers 1 and 2—are able to propagate into the stratosphere. Although the wave activity flux entering the stratosphere is a determining factor to explain the stratospheric state, the structure of the zonal wind in the stratosphere itself acts on the propagation of planetary waves (Lin 1982; Hartmann et al. 2000; Scott and Polvani 2004; 2006; Sigmond and Scinocca 2010). In particular, with our version of the ARPEGE-Climat GCM, Saint-Martin et al. (2011, manuscript submitted to *Climate Dyn.*) suggested that the intensity and position of the polar night jet could modulate the troposphere–stratosphere propagation channel of stationary waves. Consequently, as the winter stratospheric jet acts as a waveguide, the wave–mean flow interaction in the stratosphere results from a competing mechanism by which the zonal wind structure and the planetary waves influence each other.

To examine the impact of our nudging methodology on the planetary wave activity in the Northern Hemisphere, Fig. 2 shows the climatological vertical component of the WAF at 150 hPa for the ERA-40 (Fig. 2a), the CTL experiment (Fig. 2b), the bias in CTL (Fig. 2c), and the difference between CTL and CTLN (Fig. 2d). The model is able to capture the main sources of stationary waves observed over the North Pacific–Siberia region

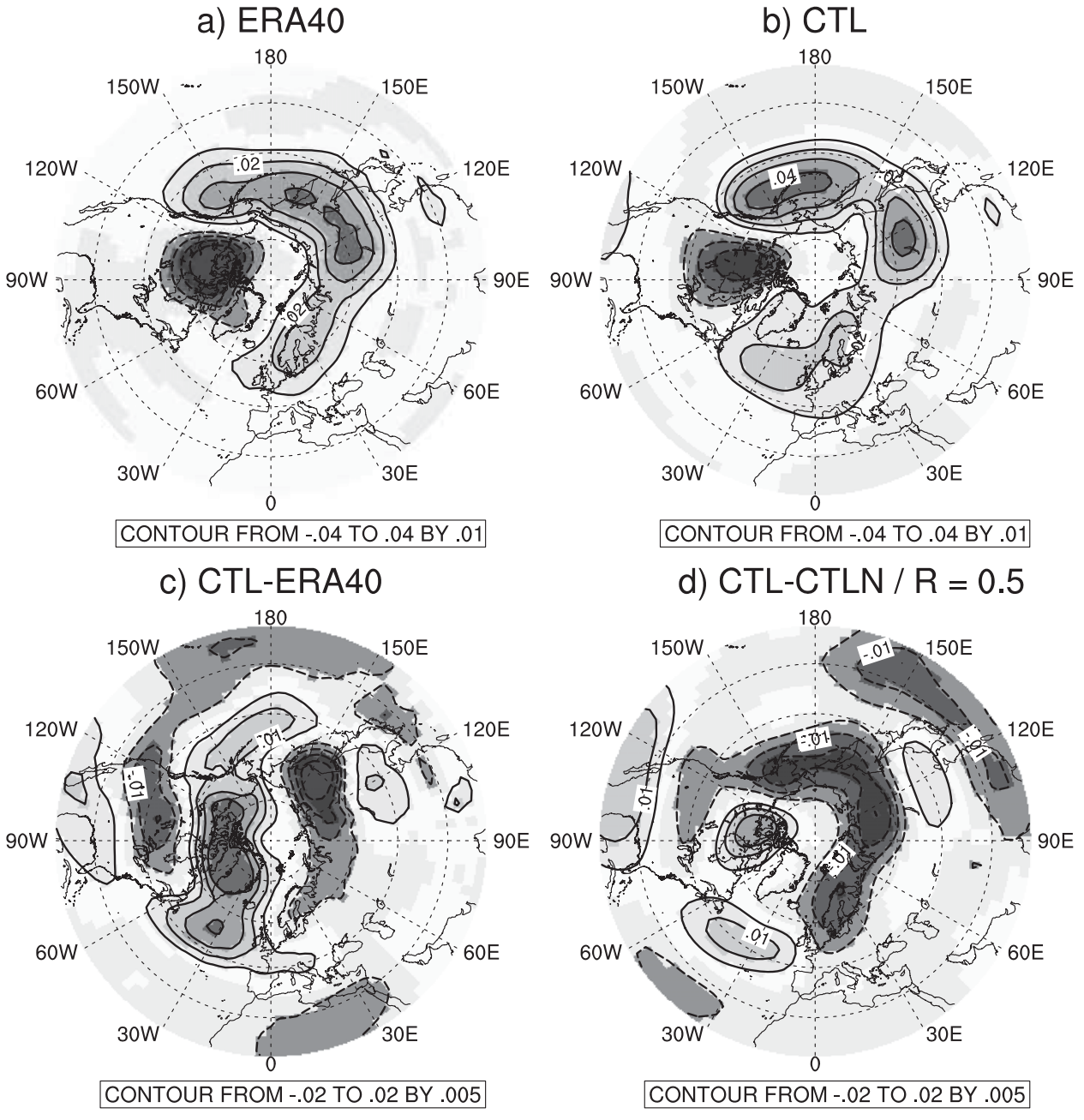

FIG. 2. Climatology of the vertical component of the winter (DJF) WAF at 150-hPa level, over the 1971–2000 period for (a) ERA-40 and (b) the CTL experiment. (c) Bias of the CTL experiment compared to ERA-40. (d) Differences between the CTL and the CTLN experiments (CTL − CTLN). The correlation *R* between the anomalies maps (c) and (d) is indicated.

and the North Atlantic (Plumb 1985), and the sink of WAF over North America. However, Fig. 2c shows that some biases are important, such as the lack of upward WAF over Siberia. The difference CTLN − CTL (Fig. 2d) illustrates the effect of a better representation of the polar vortex on the wave propagation. The upward WAF component is significantly modified over broad regions of the Northern Hemisphere. The new zonal wind climatology mostly enhances the climatological sources and sinks, which are too weak in the control experiment. In particular, it favors a stronger upward propagation of waves over our region of interest, namely, the North Pacific–Siberia region. The spatial correlation of 0.5 between Figs. 2c and 2d confirms that the WAF climatology is closer to the reanalyses in the CTLN experiment. These results are consistent with the

studies of Lin (1982) and Saint-Martin et al. (2011, manuscript submitted to *Climate Dyn.*), which suggest that a more northward position of the winter polar night jet leads to more troposphere–stratosphere upward wave propagation.

d. Snow perturbation method

As discussed previously, the equatorial stratosphere relaxation has a significant influence on the extratropical stratosphere climatology. Consequently, we chose to design two sensitivity experiments: one [snow boundary anomaly (SBA)] with the standard version of the ARPEGE-Climat model, the other [snow boundary anomaly with nudging (SBAN)] with an improved climatology of the polar vortex associated with the nudging of the equatorial stratosphere. These two sensitivity experiments are described in Table 1, and are associated with the CTL and CTLN control runs, respectively. They are also driven by climatological SST, and each experiment is a 50-member ensemble with independent initial conditions from the appropriate control run (CTL for SBA and CTLN for SBAN). The same snow forcing is added in both sensitivity experiments: a snow mass anomaly of 100 kg m^{-2} is prescribed over Siberia (see Fig. 3a for the domain) and is held constant throughout the entire run, from 1 October to 31 March. This perturbation is equivalent to that prescribed by F09 in their sensitivity experiments. However, it should be noted that their deep snow experiment is compared with another perturbed experiment in which the snow is held to its 1 October value, while we compare our simulation to a control one with freely varying snow. In this sense, our study cannot be compared exactly with their results.

TABLE 1. List and description of experiments.

Name	Description
Without nudging (interactive equatorial stratosphere)	
CTL	Control run 1950–2000
SBA	100 kg m^{-2} snow anomaly prescribed over Siberia from 1 Oct to 31 Mar (50 members)
With nudging (ERA-40-relaxed equatorial stratosphere)	
CTLN	Control run 1950–2000
SBAN	100 kg m^{-2} snow anomaly prescribed over Siberia from 1 Oct to 31 Mar (50 members)

3. Results

a. Free sensitivity experiment (SBA-CTL)

Before we look at the response of the winter extratropical circulation, it is interesting to consider how the prescribed snow anomaly perturbs the surface climate in October. This is illustrated in Fig. 3. The positive snow anomaly increases the surface albedo by about 20% over the Siberian domain. It results in strong cooling of the lower troposphere (up to midtroposphere, not shown) with a more pronounced decrease of the temperature in the southern part of Siberia (~6 K), where the incoming solar radiation is still fairly high in autumn. This strong cooling results in a strengthening of the Siberian high, extending beyond the perturbed region over southeastern Eurasia. In line with previous studies (Walsh and Ross 1988; Walland and Simmonds 1997), the anomalous high over Siberia is associated with negative anomalies on both sides and, in particular, with an enhanced Aleutian low over the North Pacific.

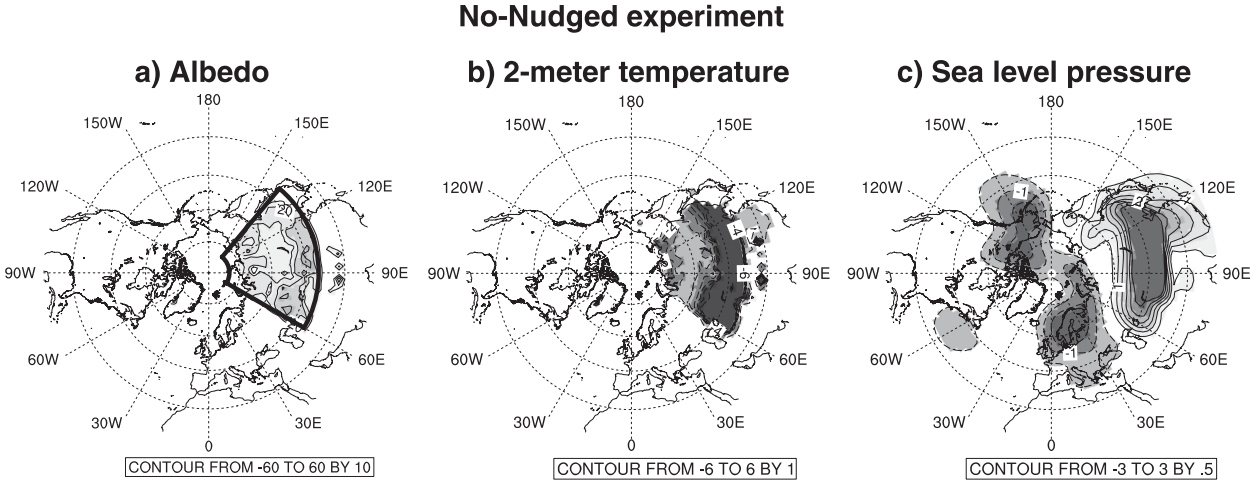

FIG. 3. Anomalies SBA-CTL in October for (a) surface albedo (%), (b) 2-m temperature (°K), and (c) sea level pressure (hPa). In (a), thick lines indicate the snow anomaly area.

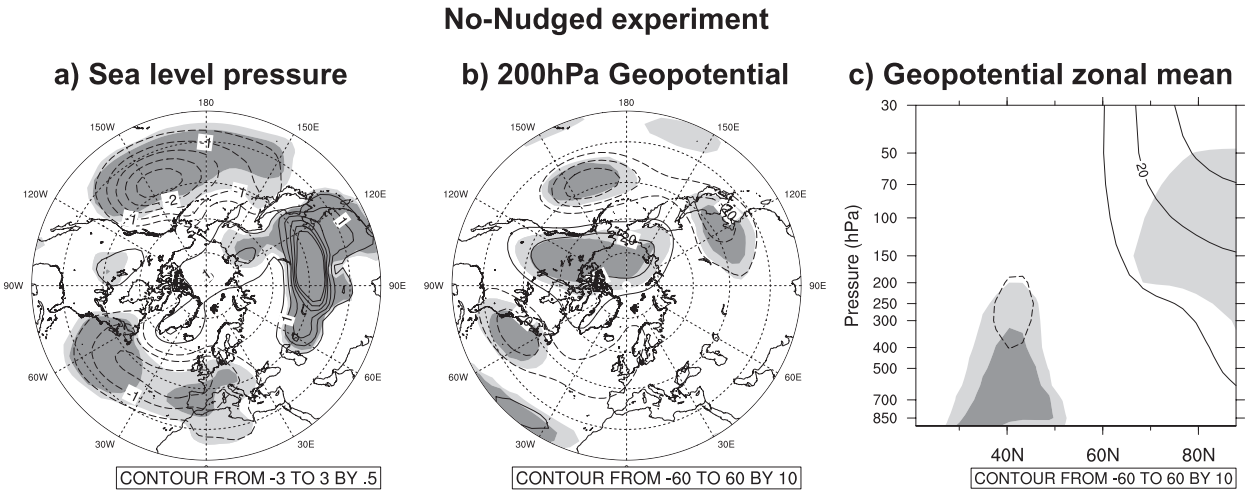

FIG. 4. Anomalies SBA-CTL in winter (December–March) for (a) sea level pressure (hPa), (b) 200-hPa geopotential (m), and (c) geopotential zonal mean (m). Light (dark) shading indicates the 95% (99%) significance level.

Figure 4 shows the winter (December–March) atmospheric circulation anomalies caused by the snow perturbation. The sea level pressure field is strongly modified, with persistence of the anomalous high over Siberia and two strong negative anomalies of sea level pressure over the North Pacific and North Atlantic basins (Fig. 4a). This pattern is reminiscent of the negative phase of the Arctic Oscillation but with a weak signal around the North Pole, where the positive anomaly is not significant at the 95% confidence level. The 200-hPa geopotential field highlights the barotropic nature of the anomalies located over the North Pacific and Atlantic regions, and suggests a more pronounced response of the polar cap region at the tropopause (Fig. 4b). The vertical distribution of the zonal-mean geopotential anomalies (Fig. 4c) indicates increased geopotential heights north of 60°N over the major part of the atmospheric column, suggesting a weakened polar vortex. While this result is in qualitative agreement with previous modeling studies (G03; F09), the weakening of the polar vortex is limited and is only significant in the lower stratosphere. Consequently, the midlatitude response resembles that obtained by former studies, while the polar cap response is weaker and does not show a clear AO response at the surface. Despite this difference, the modeled tropospheric response is quite strong and confirms the hemispheric influence of the Siberian snow on the winter atmospheric circulation.

Given the weak sensitivity of the polar vortex in this experiment, it seems that the mechanism involved is not the same as that proposed by C07 and found by G03 and F09 in their sensitivity experiments. To understand this mechanism, Fig. 5 shows the WAF and zonal wind anomalies for the autumn/early winter [October–December (OND)] and the late winter [January–March (JFM)], together with the WAF divergence (gray contours). Figures 5a and 5c allow us to characterize the stratospheric response at 50 hPa, while Figs. 5b and 5d illustrate the vertical structure of the anomalies on zonal mean for wind and over the Siberian region (between 60° and 180°E) for WAF. We focus on the Siberian sector for WAF as a zonal mean masks the signal, the strongest response being located in this region.

During OND, we observe an increased southeastward activity of stationary waves over Siberia at 50 hPa (Fig. 5a) corresponding to an upward flux to the south of the snow anomaly (Fig. 5b). The anomalous waves do not propagate toward the stratosphere but are reflected equatorward and propagate into the subtropical upper troposphere. In line with the Eliassen and Palm (1961) theory, the divergence of the stationary waves is associated with an acceleration of the zonal wind, leading to a strengthening of the Asian subtropical jet. The subtropical jet response is consistent with a stronger meridional temperature gradient to the south of the perturbed region (not shown), which is associated, under the thermal wind rule, with an increase of the westerlies at altitude. An anomalous propagation of stationary waves is also discernible over North America, from the North Pacific region toward the North Atlantic basin, which will be shown to persist in winter and will be further discussed below.

During JFM, the polar night jet is slightly weakened over the Siberia–Pacific sector (Fig. 5c), in association with the persistence of the anomalous wave activity over Siberia and the strong subtropical jet (Fig. 5d). The zonal wind negative anomaly is found over the entire atmospheric column but is relatively weak, highlighting that the hemispheric response obtained in Fig. 4 cannot be

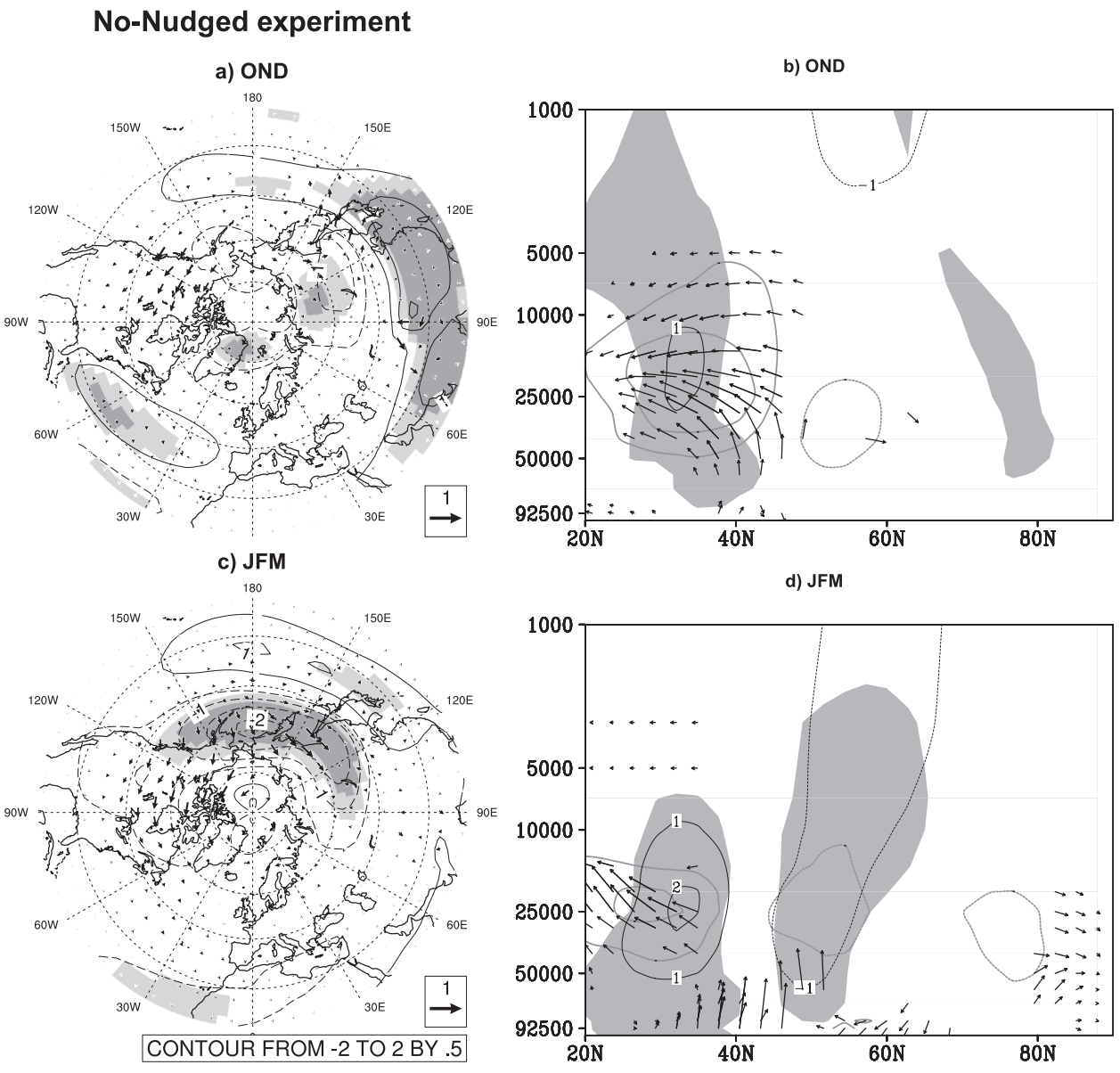

FIG. 5. Anomalies SBA-CTL in early season (OND) for (a) the zonal wind and horizontal WAF component at 50 hPa. Light (dark) shading indicates the 95% (99%) significance level. (b) Zonal-mean zonal wind (black contour), zonal mean of WAF ($m^2\ s^{-2}$) over Siberia (60°–180°E), and its divergence (gray contours). Only anomalies significant at the 95% confidence level are shown for WAF, and shading indicates the 95% significance level for zonal wind anomalies. (c),(d) As in (a),(b), respectively, for the late season (JFM). Longest meridional vector is 5 $m^2\ s^{-2}$; longest vertical vector is 0.05 $m^2\ s^{-2}$.

attributed essentially to a stratospheric pathway involving the polar vortex. Interestingly, the horizontal wave activity is again abnormally high over North America (Fig. 5c), from the Aleutian low to the North Atlantic region. This result suggests that, in this experiment, the atmospheric perturbation induced by snow propagates horizontally, from Siberia to the North Pacific, then from the North Pacific to the North Atlantic. The mechanism is thus very different from those proposed by C07, which mainly involve a vertical propagation of the zonal wind anomalies to explain the snow–AO teleconnection. It is reminiscent of works by Orsolini and Kvamstø (2009), who used the ARPEGE-Climat GCM to study the role of the Eurasian snow cover in wintertime circulation. Their study suggests that the variability in the extent of autumn–early winter snow cover over eastern Eurasia is linked to circulation anomalies over the North Pacific that influence the North Atlantic sector in late winter through the development of the Aleutian–Icelandic low seesaw (AIS). The main difference is that this teleconnection

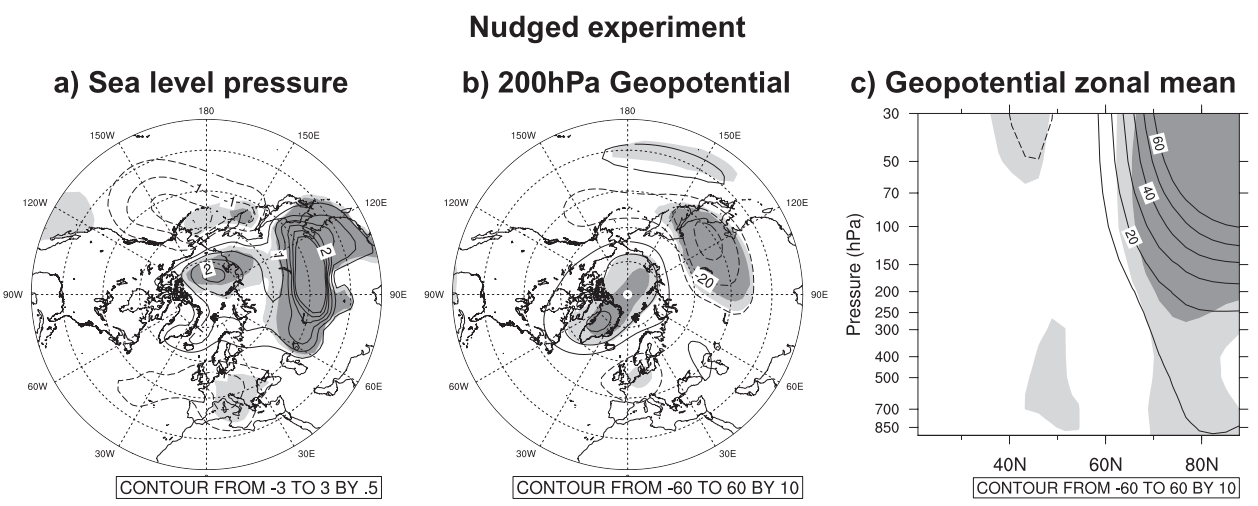

FIG. 6. As in Fig. 4, but for the nudged experiment (SBAN-CTLN anomalies).

occurs in the first months of our runs (see section 3c for more details), while it operated in late winter in Orsolini and Kvamstø (2009). This difference could be related to the forcing, which is more intense in our experiment since they prescribed observed snow cover anomalies in the model.

The results of our sensitivity experiment are, however, questionable given the poor climatology of the winter polar vortex in the control experiment. Comparing these results with those obtained from the nudged experiment will now allow us to evaluate how the model climatology of the extratropical stratosphere modulates the response to the snow perturbation and whether the new response is more consistent with the observed one.

b. Nudged sensitivity experiment (SBAN-CTLN)

In the nudged experiment, the October anomalies (albedo, 2-m temperature, sea level pressure) (not shown) are very close to those depicted in Fig. 3, suggesting that the stratospheric climatology does not influence the local and early response to the Siberian snow forcing. However, concerning the winter anomalies, Fig. 6 shows some striking differences. First, the negative surface AO pattern (Fig. 6a) is characterized by a more pronounced positive anomaly over the polar cap and by weaker anomalies over the Atlantic and Pacific basins. This feature is also found at 200 hPa (Fig. 6b), where the main signal, apart from the baroclinic local response, is seen in the North Pole region. The difference with the no-nudged experiments is even more marked on the geopotential zonal mean (Fig. 6c). The weakening of the polar vortex is more pronounced than in SBA-CTL: the amplitude of the anomaly is twice as high and it is significant over the entire atmospheric column, in line with the surface pattern (Fig. 6a). Thus, when the polar vortex climatology is more realistic, the Siberian snow perturbation seems to modulate the winter atmospheric circulation in a different way, with a higher sensitivity of the polar cap and a more limited influence over the midlatitude regions.

To understand what mechanism explains the differences between the two types of simulations, Fig. 7 depicts the same diagnostics as Fig. 5, that is, the WAF and zonal wind anomalies for autumn–early winter (OND) and late winter (JFM). From the start of the run, the polar night jet weakening is clearly greater than in Fig. 5a and extends over the whole hemisphere at 60°N (Fig. 7a). It is associated with a notable WAF anomaly over Siberia (Fig. 7b), which is more intense than in the free sensitivity experiment. In addition to the equatorward propagation and subtropical divergence of the WAF, we now observe significant WAF anomalies in the mid- and high-latitude stratosphere and a weakening of the polar night jet. These zonal wind anomalies are related to a large convergence zone located in the lower stratosphere (gray contours).

The marked weakening of the polar vortex persists until late winter, as does the anomalous WAF over Siberia (Figs. 7c and 7d). Compared to the free experiment (Figs. 5c and 5d), the anomalous stationary waves are stronger and are now able to propagate into the extratropical stratosphere. Thus, they decelerate the polar night jet more efficiently, leading to stratospheric zonal wind anomalies that propagate downward into the troposphere. The following feedback mechanism could explain the changes in wave–mean flow interactions from SBA-CTL to SBAN-CTLN experiments. First, as the jet is shifted poleward, it is more sensitive to planetary waves and is more easily disturbed by the snow-driven wave activity. However, the polar vortex does not play a passive role in this mechanism and, in turn, exerts an

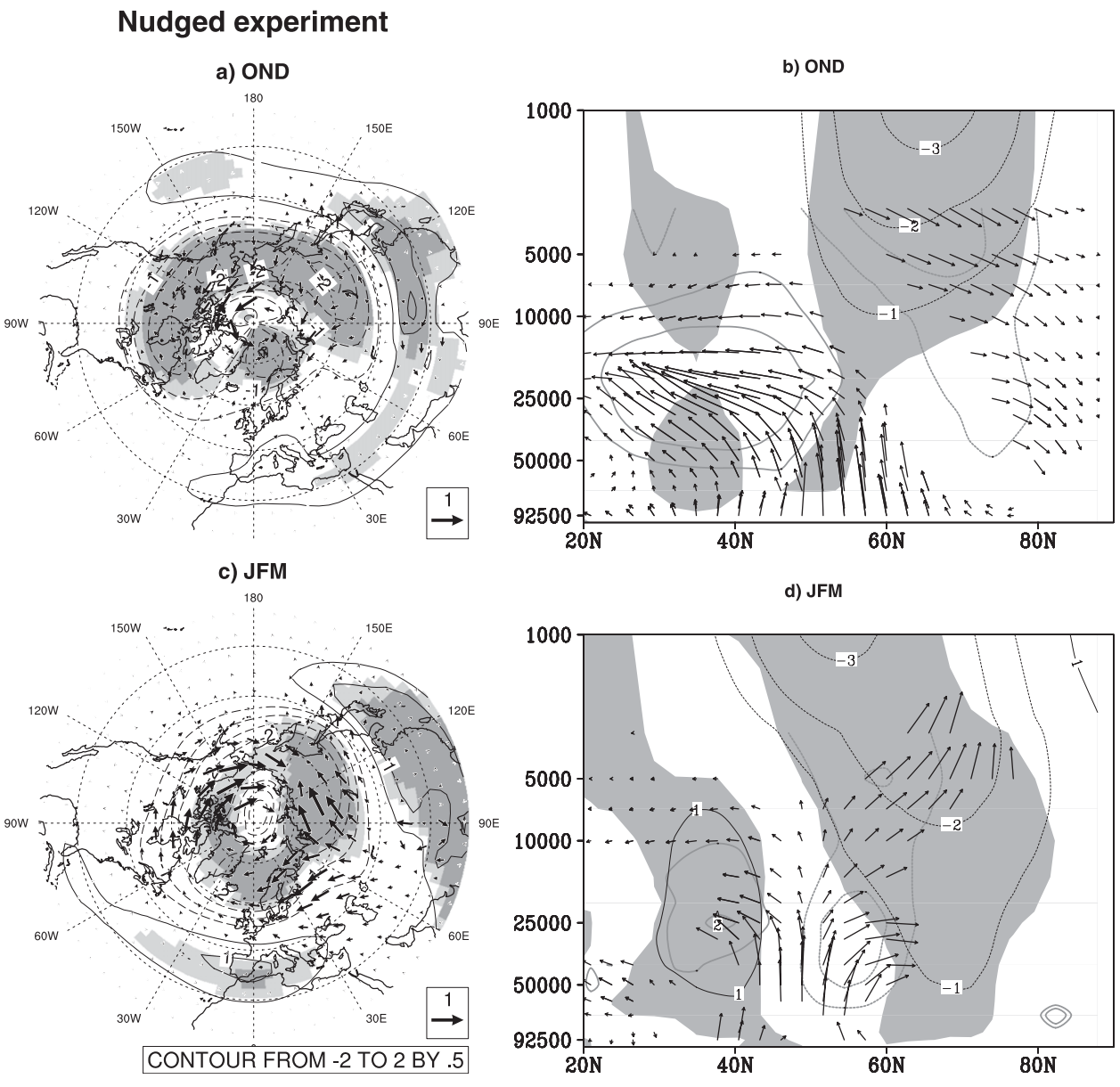

FIG. 7. As in Fig. 5, but for the nudged experiment (SBAN-CTLN anomalies).

influence on the wave propagation, as discussed in section 2c. We found that, for a given snow perturbation, a more northward and stronger polar vortex led to larger stationary wave activity over Siberia and to more intense troposphere–stratosphere coupling in the extratropics.

To sum up, depending on the polar vortex climatology, the winter atmospheric response to the Siberian snow forcing can be very different. Although the snow–atmospheric pathway in the no-nudged experiments seems to involve a horizontal propagation of Rossby waves from Siberia as far as the North Atlantic region, the nudged experiments confirm the mechanism proposed by C07, the Siberian snow anomalies being able to modulate the winter polar vortex by exciting stationary waves propagating from the troposphere to the stratosphere. These zonal wind anomalies are not confined to the stratosphere: they propagate downward and lead to a negative AO-like pattern at the surface.

c. *Intraseasonal evolution of the response*

Beyond the seasonal mean anomalies, the prescribed snow perturbation has intraseasonal signatures that can be analyzed to better understand the physical mechanisms at work in our sensitivity experiments.

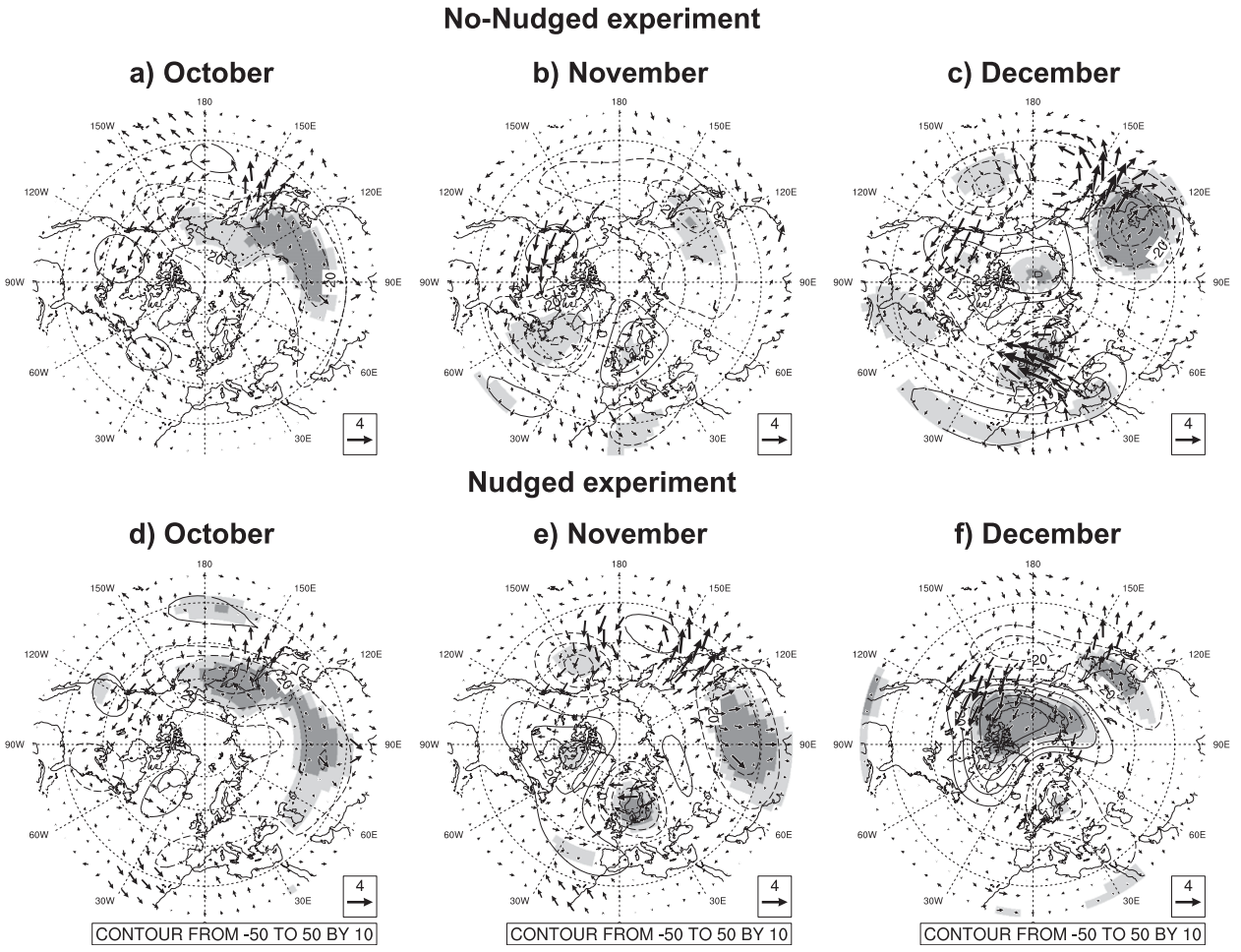

FIG. 8. Monthly anomalies in early season (OND) of the geopotential height (contours) and the horizontal WAF component at the 200-hPa level [arrows, (m^2 s^{-2})]. Light (dark) shading indicates the 95% (99%) significance level for geopotential anomalies. (a)–(c) Results for SBA-CTL; (d)–(f) Results for SBAN-CTLN.

1) NO-NUDGED EXPERIMENT

Section 3a suggests a horizontal propagation of the snow-driven atmospheric anomaly over Siberia. To give a clearer idea of the timing of this response during the run and of the horizontal propagation of planetary waves, Fig. 8a shows the geopotential and horizontal wave activity flux anomalies at 200 hPa for October, November, and December in the no-nudged experiment (SBA-CTL). To compare the response with the nudged experiment, Fig. 8b depicts the same analysis for SBAN-CTLN anomalies. The anomalies are quite similar in October for our two experiments (Figs. 8a and 8d), with the strengthening Siberian high and an eastward propagation of waves from the Pacific basin to the Atlantic over North America. In November (Figs. 8b and 8e), some differences appear, this horizontal wave propagation being reinforced over North America in the no-nudged experiment but not in the nudged one. Finally, a look at the December anomalies confirms the results from section 3a (Figs. 8c and 8f): a hemispheric wave train is clearly visible from Siberia, through North America to Europe with significant geopotential anomalies over these regions. The wave activity flux anomaly persists over North America and a Rossby wave train is now visible over Europe, associated with strong wave activity from the Mediterranean region toward the North Atlantic. Conversely, for the nudged experiment, there are no significant anomalies over the North Atlantic, either for geopotential or WAF. The wave propagation originating from the Pacific region is totally absorbed by the lower stratosphere westerly winds and leads to a weakening of the polar vortex (positive geopotential anomalies centered over the North Pole). Thus, these results corroborate the results from section 3a and confirm that seasonal anomalies of geopotential observed in SBA at the hemispheric scale are mainly related to horizontal propagation of snow-driven waves.

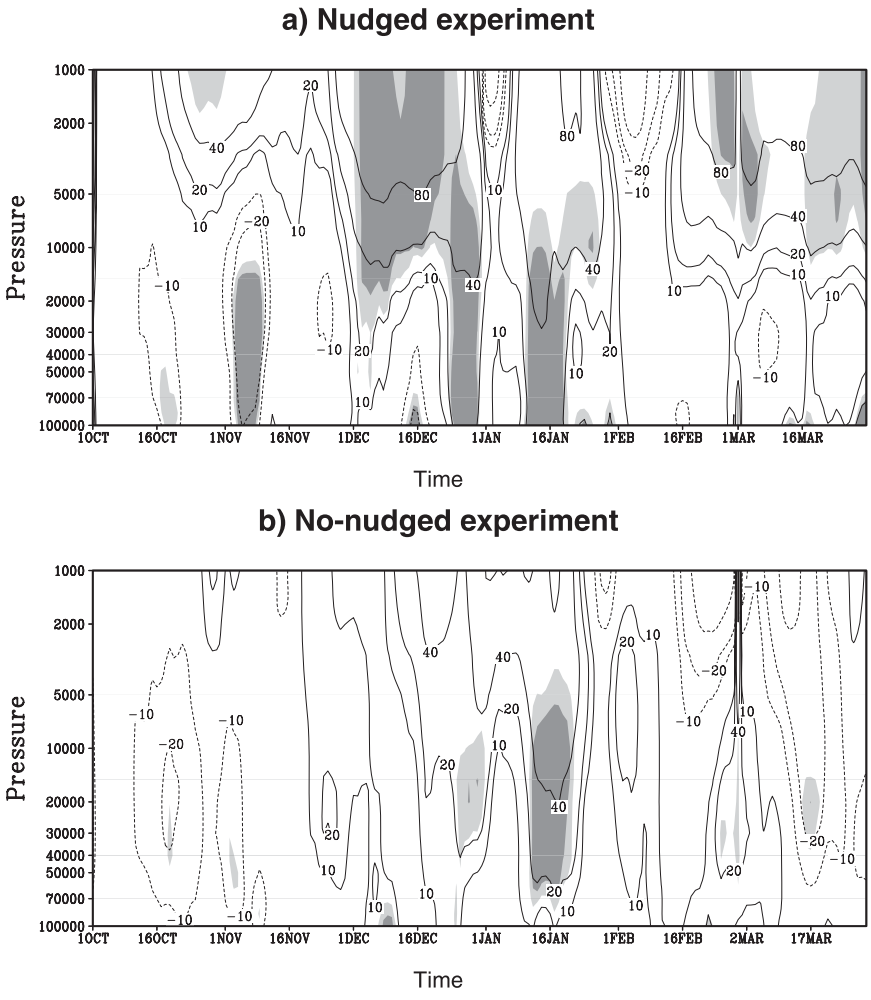

FIG. 9. Time–pressure cross section of the daily polar cap anomalies (geopotential averaged north of 60°N, m) for (a) SBAN-CTLN and (b) SBA-CTL. Light (dark) shading indicates the 95% (99%) significance level.

2) NUDGED EXPERIMENT

Section 3b showed that when the polar vortex climatology is more realistic (SBAN-CTLN), the response is in better agreement with observations and previous studies on the subject. At seasonal scale, a marked weakening of the polar vortex is simulated, associated with greater wave propagation into the polar atmosphere as in the SBA-CTL experiment. To assess how these responses impact the surface climate, it is common to plot the time–pressure cross section of the geopotential polar cap (geopotential height averaged north of 60°N at all pressure levels), which is shown in Fig. 9 for both the nudged and no-nudged sensitivity experiments. The downward propagation of the annular mode response can be followed in this plot, a positive geopotential anomaly representing a weaker polar vortex and a negative AO anomaly (and conversely). For the nudged experiment, the negative AO anomaly originates in the stratosphere at the end of October and grows much stronger in December, when it becomes statistically significant (Fig. 9a). The stratospheric anomaly then propagates downward into the troposphere, reaching the surface for the first time around 1 December and then more clearly at the end of the month. We also observe a significant surface anomaly in mid-January, but it is not preceded by a distinct downward propagation. Interestingly, significant anomalies also appear in the stratosphere at the end of the run in March. Although they do not significantly reach the surface, they suggest a signal reemergence when the radiative effect of snow on the albedo reappears in early spring. However, this effect is limited by the weak stratosphere–troposphere coupling during this season. All these results support the C07

theory, and the G03 and F09 modeling studies, though the model response is less pronounced here. Apart from differences in the experimental design (specified in section 2d), a possible explanation is that the polar vortex biases are only partly removed by the equatorial stratospheric nudging (see section 2c), so we can wonder whether the response would be even larger with a perfect stratospheric climatology.

Figure 9b shows the same diagnosis as in Fig. 9a for the free experiment. It illustrates once again the strong dependence of the results on the extratropical stratosphere climatology. The differences are striking: apart from the mid-January signal near the surface, no significant signal is present during the three first months of the run, and no stratosphere–troposphere propagation is discernible. This confirms that, although the hemispheric response in the no-nudged experiment is strong, in particular over the North Pacific and North Atlantic regions, it does not involve a stratospheric pathway as for the nudged experiment.

To follow the wave–mean flow interactions more precisely, Fig. 10 depicts the WAF and zonal wind anomalies (SBAN-CTLN) for several successive 15-day periods, from 1 October to 31 December. The anomalous wave activity over Siberia begins from the start of the runs, and becomes stronger in the second part of October (Figs. 10a and 10b), when a slight negative zonal wind anomaly appears in the stratosphere. This signal strengthens in November, with a strong WAF pulse in the second part of the month associated with a weakening of the polar vortex in the entire stratospheric column.(Figs. 10c and 10d). Whereas the strong upward WAF activity is maintained over Siberia during December, the polar vortex weakening peaks and reaches the troposphere at the end of the month (Figs. 10e and 10f). A descending branch of the WAF is visible at higher latitudes, probably related to a reflection of the planetary waves from the stratosphere to the troposphere in these regions

These results shed new light on the mechanisms at work in the model. On the one hand, they emphasize the progressive nature of the polar vortex response, which grows during the first three months of the runs. On the other hand, we observe that the wave-driven polar vortex disturbance is due to a cumulative WAF anomaly rather than to an instantaneous wave pulse, in line with the results from previous studies (Polvani and Waugh 2004; F09). These findings raise an interesting question, why does the high stationary wave activity persist during winter, whereas the radiative effect of the snow anomaly vanishes with the decreasing incident solar radiation over Siberia? A possible explanation is that the strong upward WAF propagation and the polar vortex collapse are related by a feedback mechanism: as the polar night jet appears in late autumn–early winter in the stratosphere, it acts as a waveguide for the tropospheric waves, which propagate more easily toward the stratosphere. The wave–mean flow interaction leads to a weakening of the westerly winds, again favoring greater propagation of the waves into the stratosphere, in line with the Charney–Drazin theory. This enhanced wave propagation then weakens the polar vortex even more, resulting in a downward propagation of the annular signal from the stratosphere to the troposphere (Baldwin and Dunkerton 2001).

4. Conclusions

This study revisits the well-documented relationship between the autumn Siberian snow and the winter Arctic Oscillation mode. It extends the modeling studies of G03 and F09, using the ARPEGE-Climat model and an original nudging methodology to reduce the model biases in the northern extratropics. The nudging of the equatorial stratosphere toward the ERA-40 climatology allows us to improve the meridional temperature gradient and, thereby, to simulate a more northward and more intense polar night jet. This step is crucial for our work, as the snow–AO link involves a stratospheric pathway and a polar vortex disturbance caused by snow-driven planetary waves propagating vertically from the troposphere. Moreover, it offers the possibility to discuss how the results of our snow sensitivity experiment depend on the model extratropical climatology. While a substantial fraction of the polar vortex biases have been removed, we can wonder whether the results would be different with an even better simulation of the mean winter circulation in the northern stratosphere.

Two types of sensitivity experiments are performed (''no nudged'' and ''nudged'' experiments), consisting of a 50-member ensemble with the same 100 kg m^{-2} snow anomaly prescribed over Siberia from 1 October to the end of March. Our main conclusions can be summarized as follows:

1) In the free experiment (unrealistic representation of the polar vortex), the snow perturbation causes a strong and significant hemispheric-scale response of the winter atmosphere, resembling a negative AO event. The anomalous high caused by the thermal cooling over Siberia induces Rossby wave propagation and significant negative sea level pressure anomalies over the North Pacific and North Atlantic basins. A slight weakening of the polar vortex is observed but is only significant in the lower stratosphere.

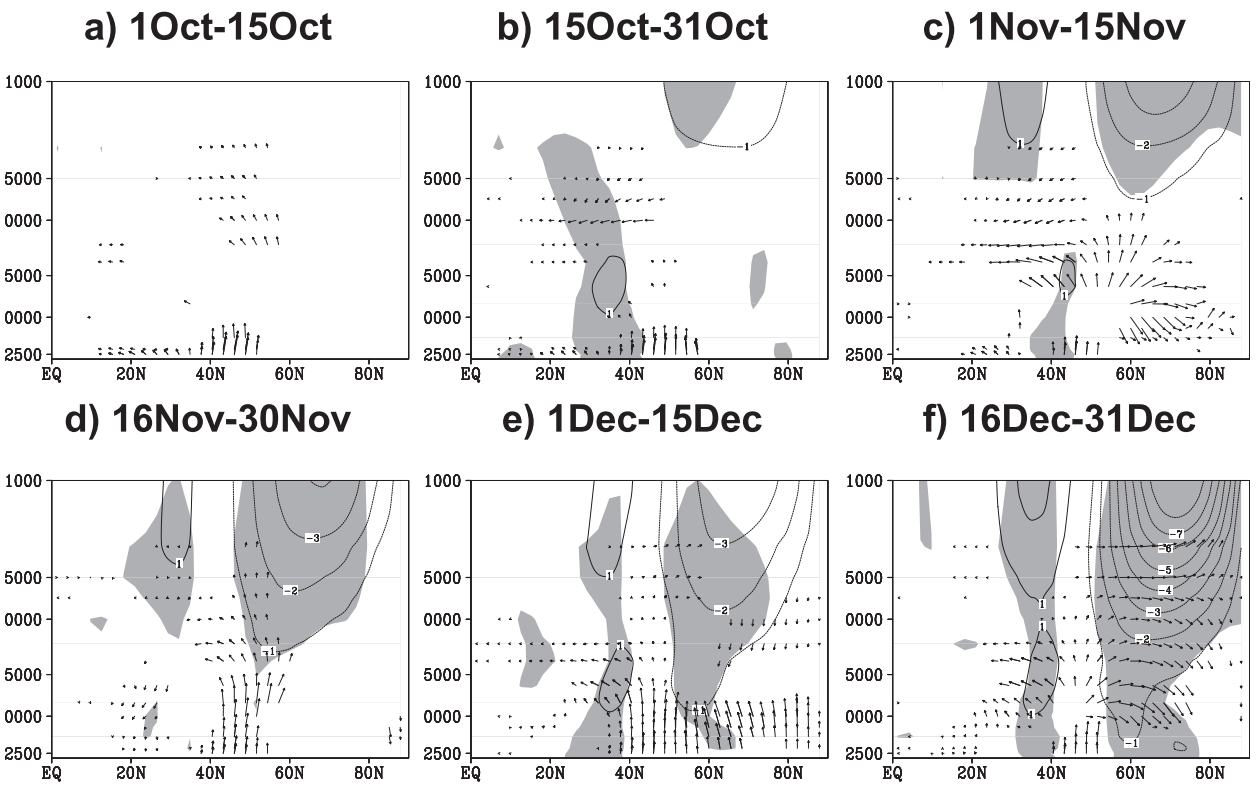

FIG. 10. Latitude–pressure cross section SBAN-CTLN anomalies for the zonal-mean zonal wind (contours, m s^{-1}) and the zonal mean of WAF (m^2 s^{-2}) over Siberia (60°–180°E). Time-averaged 15-day period: (a) 1–15 Oct, (b) 15–31 Oct, (c)1–15 Nov, (d) 15–30 Nov, (e) 1–15 Dec, and (f) 15–31 Dec. Only anomalies significant at the 95% confidence level are shown for WAF, and shading indicates the 95% significance level for zonal wind anomalies. Longest meridional vector is 5 m^2 s^{-2}; longest vertical vector is 0.05 m^2 s^{-2}.

Consequently, in contrast to the C07, G03, and F09 studies, the snow–atmospheric pathway seems to involve a horizontal propagation of the signal, rather than a vertical propagation and a strong troposphere–stratosphere interaction.

2) In the nudged experiment (more realistic polar vortex), the winter atmospheric response is close to a negative AO event too but with less pronounced anomalies over the midlatitudes and a more significant weakening of the polar vortex visible over the entire atmospheric column. The new polar night jet position favors the propagation toward the stratosphere of the snow-driven planetary waves, which are now able to weaken the polar vortex, whereas they were trapped and refracted toward the subtropics in the no-nudged experiment. The resulting polar warming is then able to propagate from the stratosphere toward the troposphere, leading to a negative AO pattern at the surface several weeks later in line with the Baldwin and Dunkerton (2001)-type events. All these results resemble those obtained by G03 and F09, and are close to the observed mechanisms described by C07. They also confirm the relevance of the stratosphere for simulating and predicting the AO and NAO wintertime variability (e.g., Douville 2009).

To sum up, our study corroborates those of Hardiman et al. (2008) by confirming the importance of a correct representation of the stratospheric mean state to capture the observed snow–AO teleconnection. As most GCMs used in seasonal forecasting present biases similar to those of the ARPEGE-Climat model, with a polar night jet that is too weak and displaced southward (Maycock et al. 2011), this probably leads to lower predictive skill of these models at the seasonal scale. Our results emphasize the need to improve the stratospheric dynamics in the climate models to enhance their predictive skill and to better understand large-scale atmospheric teleconnections. Although the nudging method is not relevant in a predictive approach, it is useful to advance our comprehension of the mechanisms involved in such atmospheric teleconnections by correcting the model biases. Concerning model development, several improvements could lead to a better representation of the winter stratospheric polar vortex. For ARPEGE-Climat, the introduction of interactive

atmospheric chemistry and higher vertical resolution in the stratosphere represent some priorities to be tested at Centre National de Recherches Météorologiques (CNRM). It will be interesting to test the model sensitivity to Siberian snow again with this new version of ARPEGE-Climat. The aim of this paper is mainly to highlight the strong dependence of the snow–AO relationship on the northern stratosphere mean state. In this sense, the article has focused mainly on the second part of the C07 mechanism (wave–mean flow interactions) and so has not addressed the first part, that is, the conditions necessary for a significant effect of snow anomalies on the winter atmospheric variability. Additional analysis (not shown) suggested a strong intermember disparity of the polar vortex response to snow forcing. F09 shows that it depends on the initial state of the polar vortex but some composite analysis did not support such a result in our model. The recent study by Smith et al. (2010) suggests another hypothesis: the negative annular mode response is forced when the snow-driven waves are in phase with the background climatological wave. These questions deserve further investigation to determine how crucial these points are in our model. Finally, another important result from our study is the horizontal propagation of the atmospheric perturbation in our no-nudged experiment. This corroborates results from Orsolini and Kvamstø (2009) about the Siberian snow influence on AIS variability. An interesting perspective would be to quantify the importance of this mechanism relative to that proposed by C07 with reanalyses and to determine under what conditions, in terms of snow forcing and atmospheric state, these teleconnections are observed.

Acknowledgments. The authors are grateful to the EAC team in charge of the development of the ARPEGE-Climat model, and in particular to Michel Déqué for the implementation of the gridpoint nudging facility within this model. Thanks are also due to Yvan Orsolini for discussions and to the anonymous reviewers for their helpful comments to improve the quality of the paper.

REFERENCES

Allen, R. J., and C. S. Zender, 2010: Effects of continental-scale snow albedo anomalies on the wintertime Arctic Oscillation. *J. Geophys. Res.,* **115,** D23105, doi:10.1029/2010JD014490.

Andrews, D. G., J. R. Holton, and C. B. Leovy, 1987: *Middle Atmosphere Dynamics*. International Geophysics Series, Vol. 40, Academic Press, 489 pp.

Baldwin, M. P., and T. J. Dunkerton, 1989: The stratospheric major warming of early December 1987. *J. Atmos. Sci.,* **46,** 2863–2884.

——, and ——, 2001: Stratospheric harbingers of anomalous weather regimes. *Science,* **244,** 581–584.

Barnett, T. P., L. Dumenil, U. Schlese, E. Roekler, and M. Latif, 1989: The effect of Eurasian snow cover on regional and global climate variations. *J. Atmos. Sci.,* **46,** 661–685.

Bojariu, R., and L. Gimeno, 2003: The role of snow cover fluctuations in multiannual NAO persistence. *Geophys. Res. Lett.,* **30,** 1156, doi:10.1029/2002GL015651.

Charney, J. G., and P. G. Drazin, 1961: Propagation of planetary-scale disturbances from the lower into the upper atmosphere. *J. Geophys. Res.,* **66,** 83–109.

Cohen, J., and D. Entekhabi, 1999: Eurasian snow cover variability and Northern Hemisphere climate predictability. *Geophys. Res. Lett.,* **26,** 345–348.

——, and C. Fletcher, 2007: Improved skill of Northern Hemisphere winter surface temperature predictions based on land–atmosphere fall anomalies. *J. Climate,* **20,** 4118–4132.

——, K. Saito, and D. Entekhabi, 2001: The role of the Siberian high in Northern Hemisphere climate variability. *Geophys. Res. Lett.,* **28,** 299–302.

——, M. Barlow, P. J. Kushner, and K. Saito, 2007: Stratosphere–troposphere coupling and links with Eurasian land surface variability. *J. Climate,* **20,** 5335–5343.

——, J. Foster, M. Barlow, K. Saito, and J. Jones, 2010: Winter 2009–2010: A case study of an extreme Arctic Oscillation event. *Geophys. Res. Lett.,* **37,** L17707, doi:10.1029/2010GL044256.

Decharme, B., and H. Douville, 2007: Global validation of the ISBA sub-grid hydrology. *Climate Dyn.,* **29,** 21–37, doi:10.1007/s00382-006-0216-7.

Déqué, M., C. Dreveton, A. Braun, and D. Cariolle, 1994: The ARPEGE/IFS atmosphere model: A contribution to the French community climate modelling. *Climate Dyn.,* **10,** 249–266.

Douville, H., 2009: Stratospheric polar vortex influence on Northern Hemisphere winter climate variability. *Geophys. Res. Lett.,* **36,** L18703, doi:10.1029/2009GL039334.

——, J.-F. Royer, and J.-F. Mahfouf, 1995: A new snow parameterization for the Météo-France climate model. Part II: Validation in a 3-D GCM experiments. *Climate Dyn.,* **12,** 37–52.

Eliassen, A., and E. Palm, 1961: *On the Transfer of Energy in Stationary Mountain Waves*. Geofysiske Publikasjoner, Vol. 22, I kommisjon hos Aschehoug, 23 pp.

Fletcher, C. G., S. C. Hardiman, P. J. Kushner, and J. Cohen, 2009: The dynamical response to snow cover perturbations in a large ensemble of atmospheric GCM integrations. *J. Climate,* **22,** 1208–1222.

Gong, G., D. Entekhabi, and J. Cohen, 2003a: Modeled Northern Hemisphere winter climate response to realistic Siberian snow anomalies. *J. Climate,* **16,** 3917–3931.

——, ——, and ——, 2003b: Relative impacts of Siberian and North American snow anomalies on the winter Arctic Oscillation. *Geophys. Res. Lett.,* **30,** 1848, doi:10.1029/2003GL017749.

——, ——, and ——, 2004a: Orographic constraints on a modeled Siberian snow–tropospheric–stratospheric teleconnection pathway. *J. Climate,* **17,** 1176–1189.

——, ——, ——, and D. A. Robinson, 2004b: Sensitivity of atmospheric response to modeled snow anomaly characteristics. *J. Geophys. Res.,* **109,** D06107, doi:10.1029/2003JD004160.

Hahn, D. J., and J. Shukla, 1976: An apparent relation between Eurasian snow cover and Indian monsoon rainfall. *J. Atmos. Sci.,* **33,** 2461–2462.

Hardiman, S. C., P. J. Kushner, and J. Cohen, 2008: Investigating the ability of general circulation models to capture the effects of Eurasian snow cover on winter climate. *J. Geophys. Res.,* **113,** D21123, doi:10.1029/2008JD010623.

Hartmann, D. L., J. M. Wallace, V. Limpasuvan, D. W. J. Thompson, and J. R. Holton, 2000: Can ozone depletion and global warming interact to produce rapid climate change? *Proc. Natl. Acad. Sci. USA,* **97,** 1412–1417.

Haynes, P. H., 2005: Stratospheric dynamics. *Annu. Rev. Fluid Mech.,* **37,** 263–293.

Honda, M., H. Nakamura, J. Ukita, I. Kousaka, and K. Takeuchi, 2001: Interannual seesaw between the Aleutian and Icelandic lows. Part I: Seasonal dependence and life cycle. *J. Climate,* **14,** 1029–1042.

Kodera, K., and M. Chiba, 1995: Tropospheric circulation changes associated with stratospheric sudden warmings: A case study. *J. Geophys. Res.,* **100,** 11 055–11 068.

Lin, B.-D., 1982: The behavior of winter stationary planetary waves forced by topography and diabatic heating. *J. Atmos. Sci.,* **39,** 1206–1226.

Matsuno, T., 1971: A dynamical model of stratospheric warmings. *J. Atmos. Sci.,* **28,** 1479–1494.

Maycock, A. C., S. P. E. Keeley, A. J. Charlton-Perez, and F. J. Doblas-Reyes, 2011: Stratospheric circulation in seasonal forecasting models: Implications for seasonal prediction. *Climate Dyn.,* **36,** 309–321, doi:10.1007/s00382-009-0665-x.

Niu, G.-Y., and Z.-L. Yang, 2007: An observation-based formulation of snow cover fraction and its evaluation over large North American river basins. *J. Geophys. Res.,* **112,** D21101, doi:10.1029/2007JD008674.

Orsolini, Y. J., and N. G. Kvamstø, 2009: Role of Eurasian snow cover in wintertime circulation: Decadal simulations forced with satellite observations. *J. Geophys. Res.,* **114,** D19108, doi:10.1029/2009JD012253.

Peings, Y., and H. Douville, 2010: Influence of the Eurasian snow cover on the Indian summer monsoon variability in observed climatologies and CMIP3 simulations. *Climate Dyn.,* **34,** 643–660, doi:10.1007/s00382-009-0565-0.

——, ——, R. Alkama, and B. Decharme, 2011: Snow contribution to springtime atmospheric predictability over the second half of the twentieth century. *Climate Dyn.,* **37,** 985–1004, doi:10.1007/s00382-010-0884-1.

Plumb, R. A., 1985: On the three-dimensional propagation of stationary waves. *J. Atmos. Sci.,* **42,** 217–229.

Polvani, L. M., and D. W. Waugh, 2004: Upward wave activity flux as a precursor to extreme stratospheric events and subsequent anomalous surface weather regimes. *J. Climate,* **17,** 3548–3554.

Saito, K., J. Cohen, and D. Entekhabi, 2001: Evolution of atmospheric response to early-season Eurasian snow cover anomalies. *Mon. Wea. Rev.,* **129,** 2746–2760.

Schlosser, C. A., and D. M. Mocko, 2003: Impact of snow conditions in spring dynamical seasonal predictions. *J. Geophys. Res.,* **108,** 8616, doi:10.1029/2002JD003113.

Scott, R. K., and L. M. Polvani, 2004: Stratospheric control of upward wave flux near the tropopause. *Geophys. Res. Lett.,* **31,** L02115, doi:10.1029/2003GL017965.

——, and ——, 2006: Internal variability of the winter stratosphere. Part I: Time-independent forcing. *J. Atmos. Sci.,* **63,** 2758–2776.

Sigmond, M., and J. F. Scinocca, 2010: The influence of basic state on the Northern Hemisphere circulation response to climate change. *J. Climate,* **23,** 1434–1446.

Smith, K. L., C. G. Fletcher, and P. J. Kushner, 2010: The role of linear interference in the annular mode response to extratropical surface forcing. *J. Climate,* **23,** 6036–6050.

Thompson, D. W. J., and J. M. Wallace, 1998: The Arctic Oscillation signature in the wintertime geopotential height and temperature fields. *Geophys. Res. Lett.,* **25,** 1297–1300.

Uppala, S. M., and Coauthors, 2005: The ERA-40 Re-Analysis. *Quart. J. Roy. Meteor. Soc.,* **131,** 2961–3012.

Walland, D. J., and I. Simmonds, 1997a: Modelled atmospheric response to changes in Northern Hemisphere snow cover. *Climate Dyn.,* **13,** 25–34.

Walsh, J. E., and B. Ross, 1988: Sensitivity of 30-day dynamical forecasts to continental snow cover. *J. Climate,* **1,** 739–754.